CHAPTER 3

Numerical Methods for Subsurface Flows and Coupling with Runoff

P. Sochala[1,*] **and A. Ern**[2]

[1] *BRGM, RNSC, 3 avenue Claude Guillemin, 45060 Orléans and*
[2] *Université Paris-Est, CERMICS, Ecole des Ponts, Champs sur Marne, 77455 Marne la Vallée, France*

Abstract: Robust and accurate schemes are proposed to couple subsurface and overland flows by enforcing the continuity of the normal flux and the pressure. Richards' equation governing the subsurface flow is discretized using a Backward Differentiation Formula in time and a symmetric interior penalty Discontinuous Galerkin method in space. The kinematic wave equation governing the overland flow is discretized using a Godunov scheme. Both schemes are individually mass conservative and can be used within coupling algorithms that ensure overall mass conservation owing to a specific design of the interface fluxes in the multi-step case. For field drainage problems, we also propose a method for representing drain tubes using Signorini type conditions. Numerical results are presented to illustrate the performances of the proposed algorithms.

Keywords: Backward Differentiation Formula, Beavers-Joseph-Saffman condition, field drainage problems, Godunov scheme, high-order initialization, hydraulic conductivity, kinematic wave equation, mass conservative schemes, matrix renumerotation, Richards' equation, saturated porous media, Signorini type conditions, subsurface flow.

1. INTRODUCTION

The interactions of subsurface and overland flows are an important ingredient to understand hydrology processes. While there is an extensive literature devoted to the numerical study of water flows in single-phase and variably saturated porous media, the issue of coupling such flows with surface flows has received less attention. A first way to couple Darcy and Stokes flows is through the well-known Beavers–Joseph–Saffman condition [1, 2]. Another approach [3] considers discontinuous pressures and evaluates an interface flux as the pressure difference multiplicated by an exchange coefficient (depending on the soil). We adopt a third approach [4, 5] based on both normal flux and pressure continuity: the hydraulic head of the subsurface flow matches the depth of the overland flow at the interface, while the normal ground flow velocity is used as a source term in the mass conservation equation of the overland flow.

In this work, the subsurface flow is described by Richards' equation and the overland flow is described by the kinematic wave approximation. Our two objectives respectively presented in Sections 2 and 3 are 1) to optimize the resolution of Richards' equation with several methods (matrix renumerotation, high-order initialization and approximation by cubic spline of the hydraulic conductivity), 2) to design robust and accurate schemes for representating drains and for coupling subsurface and overland flows in view of two physical constraints: pressure continuity and overall mass conservation.

* Address correspondence to: Pierre Sochala BRGM (French Geological Survey), 3 avenue Claude-Guillemin - BP 36009 - 45060 Orléans Cedex 2, France; E-mail: p.sochala@brgm.fr

2. RICHARDS' EQUATION

We present in this part some results concerning the resolution of the Richards' equation written in the conservative form

$$\partial_t[\theta(\psi)] - \nabla \cdot (K(\psi)\nabla(\psi + z)) = 0, \qquad (1)$$

where ψ is the hydraulic head, $\theta(\psi)$ the volumetric water content, $K(\psi)$ the hydraulic conductivity and z the vertical coordinate.

2.1. Notations

Let Ω be a bounded domain with outward normal unit vector n_Ω. The boundary of Ω is divided into the part where a Dirichlet condition $\psi = \psi_D$ is imposed and the part where a Neumann condition $-K(\psi)\nabla(\psi + z) \cdot n_\Omega = v_N$ is imposed. Let N_T be

the total number of time steps and let δt be the constant time step such that $N_T = T/\delta t$. For any integer $n \geq 0$, ψ^n denotes the value taken by ψ at time $n\delta t$. We assume that the unstationary term can be approximated by a backward differentiation formula,

$$(\partial_t[\theta(\psi)])^n = \sum_{r=0}^{q} \frac{\alpha_r^q}{\delta t}\theta(\psi^{n-r}) + \mathcal{O}(\delta t^q), \qquad (2)$$

where in (2) q is the order of the formula and $\{\alpha_r^q\}_{0\leq r\leq q}$ are suitable coefficients. The discrete functions $\left\{\psi^{n-r}\right\}_{1\leq r\leq q}$ in (2) being known, successive approximations $\psi^{n,m}$ of ψ^n are computed with a quasi-Newton procedure detailed above.

2.2. Discretization

We use a Discontinuous Galerkin (DG) method which is locally conservative, accurate and flexible in the use of non-matching meshes. The weak form of the symmetric interior penalty DG method using a BDF scheme in time and a quasi-Newton method to treat the non-linearity can be concisely written on each element τ of the mesh of size $\mathfrak{h}$ (see [6] for more details),

$$a_\tau(\psi_\mathfrak{h}^{n,m}, \delta\psi_\mathfrak{h}^{n,m}, \phi) = b_\tau(\psi_\mathfrak{h}^{n,m}, \phi),\ \forall \phi \in \mathbb{P}_p(\tau), \qquad (3)$$

where in (3) $\delta\psi_\mathfrak{h}^{n,m} = \psi_\mathfrak{h}^{n,m+1} - \psi_\mathfrak{h}^{n,m}$, the superscript m refers to the quasi-Newton loop and $\mathbb{P}_p(\tau)$ is the set of polynomials of total degree less than or equal to p on an element τ.

• The form a_τ is

$$a_\tau(\zeta,\psi,\phi) = \int_\tau \left(\frac{\alpha_0^q}{\delta t}\partial_\psi\theta(\zeta)\psi\phi + K(\zeta)\nabla\psi\cdot\nabla\phi\right)$$
$$+ \int_{\partial\tau}\left(K(\zeta|_\tau)\nabla\phi(\widehat{\psi}(\psi)-\psi) + \widehat{u}(\zeta,\psi)\phi\right)\cdot n_\tau,$$

where $\widehat{\psi}(\psi)$ is the numerical flux associated with the hydraulic head

$$\widehat{\psi}(\psi)|_F = \begin{cases} \{\psi\}_F & \text{for an internal face,} \\ 0 & \text{for a Dirichlet face,} \\ \psi & \text{for a Neumann face,} \end{cases} \qquad (4)$$

and $\widehat{u}(\zeta,\psi)$ is the numerical flux associated with the variable $u = -K(\psi)\nabla\psi$,

$$\widehat{u}(\zeta,\psi)|_F = \begin{cases} -\{K(\zeta)\nabla\psi\}_F + \eta K_s d_F^{-1}[\![\psi]\!]_F n_F, \\ -K(\zeta)\nabla\psi + \eta K_s d_F^{-1}\psi n_\Omega, \\ 0, \end{cases} \qquad (5)$$

respectively defined for an internal face, a Dirichlet face and a Neumann face. The operators $\{\}$ and $[\![]\!]$ are the average and the jump operator. The parameter η is positive (to be taken larger than a minimal threshold depending on the shape-regularity of the mesh), K_s is the hydraulic conductivity at saturation and d_F is the largest diameter of the triangle(s) of which F is a face.

• The right-hand side b_τ is

$$b_\tau(\zeta,\phi) = \int_\tau \nabla\cdot(K(\zeta)e_z)\phi - a_\tau(\zeta,\zeta,\phi)$$
$$- \int_\tau\left(\sum_{r=1}^{q}\frac{\alpha_r^q}{\delta t}\theta(\psi^{n-r}) + \frac{\alpha_0^q}{\delta t}\theta(\zeta)\right)\phi. \qquad (6)$$

For a Dirichlet face F_D, we add on b_τ the term

$$\int_{F_D}\left(-K(\zeta)\,\nabla\phi\cdot n_\Omega + \eta K_s d_F^{-1}\phi\right)\psi_D, \qquad (7)$$

and for a Neumann face F_N, we add the term

$$-\int_{F_N}(v_N + K(\zeta)e_z\cdot n_\Omega)\phi. \qquad (8)$$

2.3. Validation Test Case

We solve a one-dimensional infiltration problem in a $1m$ vertical column ($\Omega = [0,1]$) during $12h$. The soil is parametrized by the modified Van Genuchten's constitutive relations [7],

$$\theta(\psi) = \tilde{\theta}(\theta_s - \theta_r) + \theta_r, \qquad (9)$$

$$K(\psi) = K_s\tilde{\theta}^{\frac{1}{2}}\frac{\left(1-(1-(\tilde{\theta}/\beta)^{1/m})^m\right)^2}{\left(1-(1-(1/\beta)^{1/m})^m\right)^2}, \qquad (10)$$

where $\tilde{\theta}$ and β are defined as

$$\tilde{\theta} = \frac{(1+(\varepsilon h_s)^n)^m}{(1+(\varepsilon|\psi|)^n)^m} \quad \text{and} \quad \beta = (1+(\varepsilon h_s)^n)^m, \qquad (11)$$

if $\psi \leq -h_s$ and where $\tilde{\theta} = 1$ if $\psi \geq -h_s$. The parameters are

$\theta_r = 0.068$	$\theta_s = 0.38$
$K_s = 5.55\ 10^{-5}$cm s^{-1}	$\varepsilon = 0.008$ cm^{-1}
$h_s = 2$cm	$n = 1.09$
	$m = 0.0826,$

where θ_r is the residual water content, θ_s the water content at saturation and K_s the hydraulic conductivity at saturation. The parameter h_s is referred as the minimum capillary height. Figure (**1**) presents the conductivity as a function of the hydraulic head.

. Progress in Computational Physics (PiCP), Volume 2 : Coupled Fluid Flow in Energy, Biology and Environmental Research.
: Bentham Science Publishers, . p 39
http://site.ebrary.com/id/10570983?ppg=39

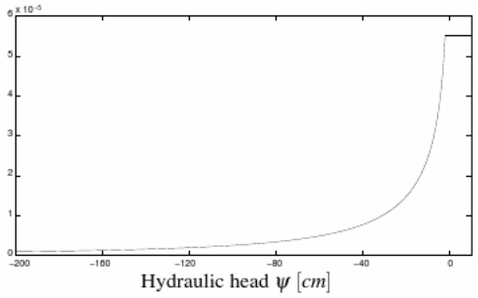

Fig. (**1**): Hydraulic conductivity.

The initial condition is an hydrostatic pressure, a zero flux is imposed on the bottom of the column and a zero hydraulic head is imposed on the top:

$$\begin{aligned} \psi^0 &= -1m - z \quad \text{in } \Omega, \\ v_N &= 0 \quad \text{at } \{0\} \times [0,T], \\ \psi_D &= 0 \quad \text{at } \{1\} \times [0,T]. \end{aligned}$$

A constant time step $\delta t = 2\text{min}$ is used. The hydraulic head plotted every 0.1 day (2h 48min) on Figure (**2**) is similar to the one in [7].

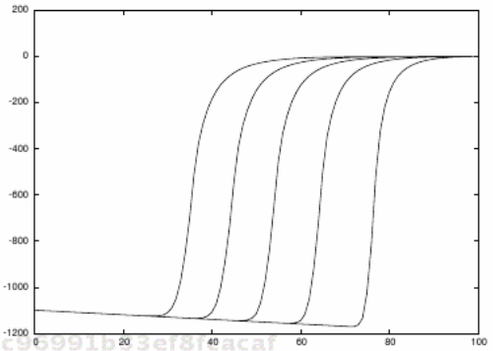

Fig. (**2**): Hydraulic head at various times.

2.4. Optimization

We study the variation of the CPU time due to the four improvements described below:
I1- a renumerotation of the non zero elements to reduce the matrix bandwith. Figure (**3**) is an example obtained with the Cuthill–McKee algorithm [8].
I2- a second-order initialization in the quasi-Newton algorithm (when the second-order BDF is used),

$$\begin{aligned} \psi_{\mathfrak{h}}^{1,0} &= \psi_{\mathfrak{h}}^{0}, \\ \psi_{\mathfrak{h}}^{2,0} &= 2\psi_{\mathfrak{h}}^{1} - \psi_{\mathfrak{h}}^{0}, \\ \psi_{\mathfrak{h}}^{n,0} &= 3\psi_{\mathfrak{h}}^{n-1} - 3\psi_{\mathfrak{h}}^{n-2} + \psi_{\mathfrak{h}}^{n-3}, \quad \forall n \geq 3, \end{aligned} \tag{12}$$

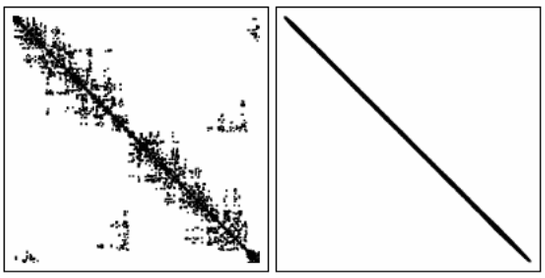

Fig. (**3**): Initial profile and ordering profile.

to replace the basic initialization $\psi_{\mathfrak{h}}^{n,0} = \psi_{\mathfrak{h}}^{n-1}$, $\forall n$.
I3- an integration by parts of the term containing the divergence of the hydraulic conductivity in b_τ,

$$\begin{aligned} \int_\tau \nabla \cdot (K(\zeta) e_z) \phi = &- \int_\tau K(\zeta) e_z \nabla \phi \\ &+ \int_{\partial\tau} K(\zeta|_\tau) e_z \, \phi \, n_\tau. \end{aligned} \tag{13}$$

I4- a cubic spline interpolation of the conductivity $\tilde{K}$ to replace K by a more simple algebraic relation.
The symbols I1, I2, I3 and I4 refer to the above improvements. Figure (**4**) shows that the relative error $e(\psi) = 100(1 - \tilde{K}(\psi)/K(\psi))$ is lower than 5% for our Van Genuchten's law interpolation (see § 2.3.).

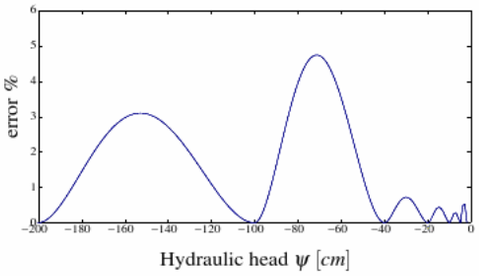

Fig. (**4**): Cubic spline interpolation error $e(\psi)$.

The quantity $\bar{N}_{it}$ is the mean number (in time) of quasi-Newton iterations and t_{CPU} is the CPU time of the simulation. The dimensionless term t^*_{CPU} is defined as

$$t^*_{\text{CPU}} = 100 \frac{t_{\text{CPU}}}{t_{\text{CPU,ref}}}, \tag{14}$$

where $t_{\text{CPU,ref}}$ is the CPU time without optimization.

It is interesting to note that the renumerotation (11) and the second-order initialisation (12) have a significant influence to the CPU time while the integration by parts (13) and the cubic spline (14) have lower impact.
As expected, $\bar{N}_{it}$ is the same when the matrix profile changes whereas $\bar{N}_{it}$ decreases when the high-order

Table 1: Optimization results.

I1	I2	I3	I4	$\bar{N}_{it}$	t_{CPU}	t^*_{CPU}
∅	∅	∅	∅	3.4	3013	100
×	∅	∅	∅	3.4	2033	67
∅	×	∅	∅	1.8	1609	53
∅	∅	×	∅	3.4	3071	102
∅	∅	∅	×	3.5	2723	90
∅	×	×	×	2.1	1610	53
×	∅	×	×	3.5	1752	58
×	×	∅	×	2.1	1106	37
×	×	×	∅	1.8	1049	35
×	×	×	×	2.1	1015	34

initialization is used. These elements permit to reduce the CPU time by a factor three.

3. COUPLING WITH RUNOFF

We present in this part the coupling of the Richards' equation with the kinematic wave (KW) approximation (this choice is made for ease of exposition and more general shallow water models can be used),

$$\partial_t h + \partial_x q = (v(\psi) - v_{\text{r}}) \cdot n_\Omega, \tag{15}$$

where h is the water depth, q the discharge, v_{r} the rainfall intensity and $v(\psi)\cdot n_\Omega$ the source or sink term resulting from mass transfer between subsurface and overland flows. The Manning–Strickler uniform flow formula is used to link the discharge and the water depth,

$$q = \mathscr{K} h^{5/3} S^{1/2}, \tag{16}$$

where $\mathscr{K}$ is the Strickler coefficient of roughness and S the bottom slope. We also consider drains in the subsurface and represent them with the following Signorini type condition,

$$\psi \le 0, \quad v(\psi)\cdot n_{\mathscr{D}} \ge 0 \quad \text{and} \quad \psi v(\psi)\cdot n_{\mathscr{D}} = 0, \tag{17}$$

where $n_{\mathscr{D}}$ is the normal to the drain boundary pointing inside the drain.

3.1. Notations

The boundary of Ω is divided into four parts: $\mathscr{I}$ is the upper part of the boundary where overland flow can occur, $\mathscr{W}$ are lateral walls, $\mathscr{B}$ represents the lower part of the boundary and $\mathscr{D}$ are drains.

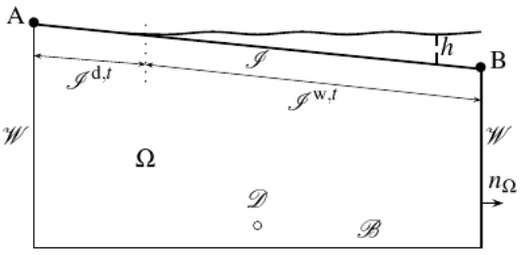

Fig. (**5**): Schematic of the computational domain.

At any time t, the set $\mathscr{I}$ is divided into "wet" and "dry" parts $\mathscr{I}^{\text{d},t} \cup \mathscr{I}^{\text{w},t}$, with

$$\begin{aligned} \mathscr{I}^{\text{w},t} &= \{x \in \mathscr{I};\ h(x,t) > 0\}, \\ \mathscr{I}^{\text{d},t} &= \{x \in \mathscr{I};\ h(x,t) = 0\}. \end{aligned} \tag{18}$$

Similarly, the set $\mathscr{D}$ is divided into "wet" and "dry" parts $\mathscr{D}^{\text{d},t} \cup \mathscr{D}^{\text{w},t}$, with

$$\begin{aligned} \mathscr{D}^{\text{w},t} &= \{x \in \mathscr{D};\ \psi(x,t) = 0\}, \\ \mathscr{D}^{\text{d},t} &= \{x \in \mathscr{D};\ \psi(x,t) < 0\}. \end{aligned} \tag{19}$$

Observe that the above partition of sets $\mathscr{I}$ and $\mathscr{D}$ are time-dependent. The total system for coupling drained subsurface flows and surface flows is

$$\begin{array}{ll}
\partial_t[\theta(\psi)] + \nabla\cdot v(\psi) = 0 & \text{in } \Omega\times[0,T], \\
v(\psi) = -K(\psi)\nabla(\psi+z) & \text{in } \Omega\times[0,T], \\
\psi(\cdot,0) = \psi^0 & \text{on } \Omega, \\
v(\psi)\cdot n_\Omega = 0 & \text{on } (\mathscr{W}\cup\mathscr{B})\times[0,T], \\
v(\psi)\cdot n_\Omega = v_{\text{r}}\cdot n_\Omega & \text{on } \{(x,t), x\in\mathscr{I}^{\text{d},t}\}, \\
\psi = h & \text{on } \{(x,t), x\in\mathscr{I}^{\text{w},t}\}, \\
v(\psi)\cdot n_\Omega = 0 & \text{on } \{(x,t), x\in\mathscr{D}^{\text{d},t}\}, \\
\psi = 0 & \text{on } \{(x,t), x\in\mathscr{D}^{\text{w},t}\}, \\
\\
\partial_t h + \partial_x q = (v(\psi) - v_{\text{r}})\cdot n_\Omega & \text{on } \mathscr{I}\times[0,T], \\
h \ge 0 & \text{on } \mathscr{I}\times[0,T], \\
h(\cdot,0) = h^0 & \text{on } \mathscr{I}, \\
h(\text{A},\cdot) = 0 & \text{at A}\times[0,T].
\end{array}$$

The coupling conditions are 1) the boundary condition $\psi = h$ on the wet part of the interface $\mathscr{I}^{\text{w},t}$ and 2) the source or sink term $v(\psi)\cdot n_\Omega$ in the mass conservation of the overland flow.

3.2. Discretization of the KW

The KW equation is discretized on the trace of the subsurface mesh on the interface $\mathscr{I}$. We use a finite volume scheme with Godunov flux and time step $\delta t'$ taken less than or equal to the time step δt for Richards' equation ($\delta t' = \delta t/n'$ with $n' \ge 1$). This choice is made because the explicit FV scheme is restricted by a CFL condition while it is not the case

for the discrete Richards' equation where a larger time step can be employed. This leads to the following notation: $h_{\mathfrak{h}}^{n,k}$ for $n \leq N_T$ and $k \leq n'$ denotes the discrete approximation of h at time $n\delta t + k\delta t'$ and for brevity we write $h_{\mathfrak{h}}^{n} = h_{\mathfrak{h}}^{n,0} = h_{\mathfrak{h}}^{n-1,n'}$. Let x_i, l_i, $x_{i-\frac{1}{2}}$ and $x_{i+\frac{1}{2}}$ be defined on a generic mesh face e_i on $\mathscr{I}$ respectively as the center, the length, and the left and right vertices of e_i (see Figure (**6**)). $N_{\mathscr{I}}$ is the number of mesh faces covering $\mathscr{I}$ and S_i denotes the slope of the face e_i. Since the flux function q is convex and the water depth is nonnegative, the Godunov flux coincides with the upwind flux, yielding $\forall k \leq n'$, $\forall i \leq N_{\mathscr{I}}$,

$$\begin{aligned} h_i^{n-1,k} &= h_i^{n-1,k-1} \\ &+ \frac{\delta t'}{l_i}\Big(q(h_{i-1}^{n-1,k-1}, S_{i-1}) - q(h_i^{n-1,k-1}, S_i)\Big) \\ &+ \frac{\delta t'}{l_i}\int_{e_i} v_{\mathfrak{h}}^{\star,n} - \delta t' v_{\mathrm{r}}^{n-1,k-1}\cdot n_\Omega, \end{aligned} \tag{20}$$

where for all $i \leq N_{\mathscr{I}}, h_i^{n,k} = h_{\mathfrak{h}}^{n,k}|_{e_i}$ and $v_{\mathfrak{h}}^{\star,n}$ is a discrete interface flux yet to be defined (see §3.3).

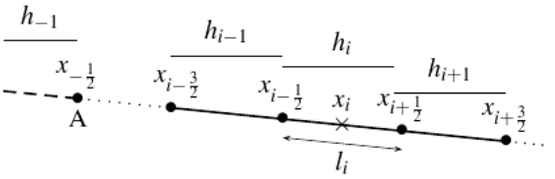

Fig. (**6**): Space discretization at the interface.

Note that a fixed interface flux is used for the multiple time steps comprised in a single time step of Richards' equation. Equation (20) requires the knowledge of the water depth at $t = 0$ and to the left of the first face on a fictitious cell at all discrete times,

$$\begin{aligned} &\forall i \leq N_{\mathscr{I}}, h_i^0 = h^0(x_i), \\ &\forall n \leq N_T, \forall k \leq n' - 1, h_{-1}^{n,k} = h_{\mathrm{A}}^{n,k}. \end{aligned} \tag{21}$$

The CFL condition for the explicit scheme (20) is

$$\delta t' \leq \frac{3}{5\mathscr{K} h_{\max}^{2/3}} \cdot \min_{1\leq i\leq N_{\mathscr{I}}} \left(l_i S_i^{-\frac{1}{2}}\right), \tag{22}$$

where $h_{\max}$ is an *a priori* bound for h on $\mathscr{I}\times[0,T]$. In the absence of rainfall and coupling terms, the satisfaction of the CFL condition implies a discrete maximum principle and a decrease in the total variation for the discrete water depth.

3.3. Coupling Algorithm

3.3.1. Presentation

For simplicity in the presentation of our coupling algorithm, we define

- $h_{\mathfrak{h}}^n \leftarrow \texttt{KW}(h_{\mathfrak{h}}^{n-1}, n', v_{\mathrm{r}}, v_{\mathfrak{h}}^{\star,n})$ as the resolution of the KW equation by using (20) n' times,
- $\{\mathscr{I}_{\mathfrak{h}}^{\mathrm{d},n,p}, \mathscr{I}_{\mathfrak{h}}^{\mathrm{w},n,p}\} \leftarrow \texttt{I\_Part}(h_{\mathfrak{h}}^{n,0}, \ldots, h_{\mathfrak{h}}^{n,p-1})$ as the partition of the interface $\mathscr{I}$,

  $$\begin{aligned} \mathscr{I}_{\mathfrak{h}}^{\mathrm{d},n,p} &= \{e_i \in \mathscr{I}_{\mathfrak{h}}, \exists k \leq p-1, h_i^{n,k} < 0\}, \\ \mathscr{I}_{\mathfrak{h}}^{\mathrm{w},n,p} &= \mathscr{I}_{\mathfrak{h}} \backslash \mathscr{I}_{\mathfrak{h}}^{\mathrm{d},n,p}, \end{aligned}$$

  where $\mathscr{I}_{\mathfrak{h}}$ is the set of faces located on $\mathscr{I}$,
- $\{\mathscr{D}_{\mathfrak{h}}^{\mathrm{d},n,p}, \mathscr{D}_{\mathfrak{h}}^{\mathrm{w},n,p}\} \leftarrow \texttt{D\_Part}(\psi_{\mathfrak{h}}^{n,0}, \ldots, \psi_{\mathfrak{h}}^{n,p-1})$ as the partition of the set $\mathscr{D}$,

  $$\begin{aligned} \mathscr{D}_{\mathfrak{h}}^{\mathrm{w},n,p} &= \{e_i \in \mathscr{D}_{\mathfrak{h}}, \psi_{\mathfrak{h}}^{n,p}|_F = 0 \\ &\qquad \text{and } \exists k \leq p-1,\ v_{\mathfrak{h}}^{\star,n,k}|_F \geq 0\}, \\ \mathscr{D}_{\mathfrak{h}}^{\mathrm{d},n,p} &= \mathscr{D}_h \backslash \mathscr{D}_{\mathfrak{h}}^{\mathrm{w},n,p}, \end{aligned}$$

  where $\mathscr{D}_{\mathfrak{h}}$ is the set of faces located on $\mathscr{D}$,
- $\{\omega_v^{n,p}, \omega_\psi^{n,p}\} \leftarrow \texttt{I\_BC}(\tilde{h}_{\mathfrak{h}}^n, \mathscr{I}_{\mathfrak{h}}^{\mathrm{d},n,p}, \mathscr{I}_{\mathfrak{h}}^{\mathrm{w},n,p})$ as the evaluation of the boundary condition on $\mathscr{I}$,

  $$\begin{aligned} \omega_v^{n,p} &= -(3\tilde{h}_{\mathfrak{h}}^n/\delta t + v_{\mathfrak{h}}^{\star,n-1})/2 \text{ on } \mathscr{I}_{\mathfrak{h}}^{\mathrm{d},n,p}, \\ \omega_\psi^{n,p} &= \tilde{h}_{\mathfrak{h}}^n \text{ on } \mathscr{I}_{\mathfrak{h}}^{\mathrm{w},n,p}, \end{aligned}$$

- $\psi_{\mathfrak{h}}^n \leftarrow \texttt{Ric\_BDF2}(\mathscr{I}_{\mathfrak{h}}^{\mathrm{d},n}, \mathscr{I}_{\mathfrak{h}}^{\mathrm{w},n}, \omega_v^n, \omega_\psi^n)$ as the resolution of Richards' equation on a time step by the SIPG method, the second-order BDF and boundary data on $\mathscr{I}$ determined from $\{\mathscr{I}_{\mathfrak{h}}^{\mathrm{d},n}, \mathscr{I}_{\mathfrak{h}}^{\mathrm{w},n}, \omega_v^n, \omega_\psi^n\}$,
- $v_{\mathfrak{h},\mathscr{E}}^{\star,n} \leftarrow \texttt{Velocity}(\mathscr{E}_{\mathfrak{h}}^{\mathrm{d},n}, \mathscr{E}_{\mathfrak{h}}^{\mathrm{w},n}, \omega_v^n, \omega_\psi^n)$ as the evaluation of the normal velocity $v_{\mathfrak{h}}^{\star,n}$ on $\mathscr{E}$ ($= \mathscr{I}$ or $\mathscr{D}$). For a face F, this velocity is defined as

  $$\begin{aligned} v_{\mathfrak{h},\mathscr{E}}^{\star,n} &= \omega_v^n|_F \text{ if } F \in \mathscr{E}_{\mathfrak{h}}^{\mathrm{d},n}, \\ v_{\mathfrak{h},\mathscr{E}}^{\star,n} &= v(\psi_{\mathfrak{h}}^n|_F)\cdot n_\Omega \\ &\quad + \eta K_s d_F^{-1}(\psi_{\mathfrak{h}}^n - \omega_\psi^n)|_F \text{ if } F \in \mathscr{E}_{\mathfrak{h}}^{\mathrm{w},n}. \end{aligned}$$

The expression for $v_{\mathfrak{h}}^{\star,n}$ on $\mathscr{E}_{\mathfrak{h}}^{\mathrm{w},n}$ corresponds to the normal component of the $H(\mathrm{div},\Omega)$-conforming velocity reconstruction derived in [9] for DG methods.

Algorithm 1 Coupling algorithm

Require: $\psi_{\mathfrak{h}}^{n-1}$ and $h_{\mathfrak{h}}^{n-1}$

$\tilde{h}_{\mathfrak{h}}^{n} \leftarrow \texttt{KW}(h_{\mathfrak{h}}^{n-1}, n', v_{\mathrm{r}}^{n-1}, 0)$

Set $p = 0$ and $h_{\mathfrak{h}}^{n,0} = \tilde{h}_{\mathfrak{h}}^{n}$,

Set $\psi_{\mathfrak{h}}^{n,0}|_{\mathscr{D}} = 0$ and $v_{\mathfrak{h},\mathscr{D}}^{\star,n,0} = 0$,

repeat

$p \leftarrow p+1$

$\{\mathscr{I}_{\mathfrak{h}}^{\mathrm{d},n,p}, \mathscr{I}_{\mathfrak{h}}^{\mathrm{w},n,p}\} \leftarrow \texttt{I\_Part}(h_{\mathfrak{h}}^{n,0}, \ldots, h_{\mathfrak{h}}^{n,p-1})$

$\{\mathscr{D}_{\mathfrak{h}}^{\mathrm{d},n,p}, \mathscr{D}_{\mathfrak{h}}^{\mathrm{w},n,p}\} \leftarrow \texttt{D\_Part}(\psi_{\mathfrak{h}}^{n,0}, \ldots, \psi_{\mathfrak{h}}^{n,p-1})$

$\{\omega_{v}^{n,p}, \omega_{\psi}^{n,p}\} \leftarrow \texttt{I\_BC}(\tilde{h}_{\mathfrak{h}}^{n}, \mathscr{I}_{\mathfrak{h}}^{\mathrm{d},n,p}, \mathscr{I}_{\mathfrak{h}}^{\mathrm{w},n,p})$

$\psi_{\mathfrak{h}}^{n,p} \leftarrow \texttt{Ric\_BDF2}(\mathscr{I}_{\mathfrak{h}}^{\mathrm{d},n,p}, \mathscr{I}_{\mathfrak{h}}^{\mathrm{w},n,p}, \omega_{v}^{n,p}, \omega_{\psi}^{n,p})$

$v_{\mathfrak{h},\mathscr{I}}^{\star,n,p} \leftarrow \texttt{Velocity}(\mathscr{I}_{\mathfrak{h}}^{\mathrm{d},n,p}, \mathscr{I}_{\mathfrak{h}}^{\mathrm{w},n,p}, \omega_{v}^{n,p}, \omega_{\psi}^{n,p})$

$v_{\mathfrak{h},\mathscr{D}}^{\star,n,p} \leftarrow \texttt{Velocity}(\mathscr{D}_{\mathfrak{h}}^{\mathrm{d},n,p}, \mathscr{D}_{\mathfrak{h}}^{\mathrm{w},n,p}, 0, 0)$

$\forall\, F \in \mathscr{I}_{\mathfrak{h}}$,

$h^{n,p}|_F = \tilde{h}^{n}|_F + \delta t/|F| \int_F (2v_{\mathfrak{h},\mathscr{I}}^{\star,n,p} + v_{\mathfrak{h},\mathscr{I}}^{\star,n-1})/3$

until 1 - $\forall\, F \in \mathscr{I}_{\mathfrak{h}}, h^{n,p}|_F \geq 0$

2 - $\forall\, F \in \mathscr{D}_{\mathfrak{h}}, v_{\mathfrak{h},\mathscr{D}}^{\star,n,p}|_F \geq 0$

Ensure: $\psi_{\mathfrak{h}}^{n} = \psi_{\mathfrak{h}}^{n,p}$ and $h_{\mathfrak{h}}^{n} = h_{\mathfrak{h}}^{n,p}$

3.3.2. Principle

1. *Initial partition*

   a) The water depth, predicted without subsurface coupling term ($v_{\mathfrak{h}}^{\star,n} = 0$) and denoted $\tilde{h}_{\mathfrak{h}}^{n}$, serves as a Dirichlet boundary condition for Richards' equation. As the Godunov scheme satisfies a discrete maximum principle, $\tilde{h}_{\mathfrak{h}}^{n}$ is nonnegative on the interface, so that $\mathscr{I}_{\mathfrak{h}}^{\mathrm{d},n,1} = \emptyset$ and $\mathscr{I}_{\mathfrak{h}}^{\mathrm{w},n,1} = \mathscr{I}$.

   b) We assume that the hydraulic head and the normal velocity are nul on the drains, so that $\mathscr{D}_{\mathfrak{h}}^{\mathrm{d},n,1} = \emptyset$ and $\mathscr{D}_{\mathfrak{h}}^{\mathrm{w},n,1} = \mathscr{D}$.

   That is, we begin the iterations by assuming that $\mathscr{I}$ and $\mathscr{D}$ are totally wet.

2. *Determination of ψ and h*

   Richards' equation is solved and a first estimate of the normal velocity $v_{\mathfrak{h},\mathscr{I}}^{\star,n,p}$ is used to evaluate the water depth $h_{\mathfrak{h}}^{n,p}$ as follows

$$h^{n,p}|_F = \tilde{h}^{n}|_F + \delta t/|F| \int_F (2v_{\mathfrak{h},\mathscr{I}}^{\star,n,p} + v_{\mathfrak{h},\mathscr{I}}^{\star,n-1})/3.$$

   The coupling term $(2v_{\mathfrak{h},\mathscr{I}}^{\star,n,p} + v_{\mathfrak{h},\mathscr{I}}^{\star,n-1})/3$ is specially design to have overall mass conservation when the second-order BDF is used for time discretization of the Richards' equation [6].

3. *New partition and Neumann condition on $\mathscr{I}$*

   a) The sign of $h_{\mathfrak{h}}^{n,p}$ is then checked on the faces of $\mathscr{I}$. If $h_i^{n,p}$ is nonnegative on all faces, the partition can be accepted. Otherwise, a new partition of $\mathscr{I}$ is determined and a Neumann condition is enforced on those faces where the water depth is negative. This Neumann condition is evaluated in such a way that 1) the surface water is completely infiltrated into the soil and 2) overall water volume conservation holds true, so that for the BDF2,

$$\omega_{v}^{n,p} = -(3\tilde{h}_{\mathfrak{h}}^{n}/\delta t + v_{\mathfrak{h}}^{\star,n-1})/2. \qquad (23)$$

   b) The sign of $v_{\mathfrak{h},\mathscr{D}}^{\star,n,p}$ is also checked on the faces of $\mathscr{D}$. A Neumann condition is imposed on the faces where $v_{\mathfrak{h},\mathscr{D}}^{\star,n,p} < 0$.

4. *Convergence*

   The hydraulic head and the water depth are accepted as the solution to the coupled system if the water depth is nonnegative on all faces of $\mathscr{I}$ and if the normal velocity is nonnegative on all faces of $\mathscr{D}$. Convergence occurs since the sets $\mathscr{I}_{\mathfrak{h}}^{\mathrm{d},n,p}$ and $\mathscr{D}_{\mathfrak{h}}^{\mathrm{d},n,p}$ increase with p while the sets $\mathscr{I}_{\mathfrak{h}}^{\mathrm{w},n,p}$ and $\mathscr{D}_{\mathfrak{h}}^{\mathrm{w},n,p}$ decrease.

3.3.3. Properties

An important point is that our algorithm delivers nonnegative surface water depths. Indeed, on the wet part of the interface, there holds

$$\forall n \leq N_T, \quad \forall F \in \mathscr{I}_{\mathfrak{h}}^{\mathrm{w},n}, \quad \psi_{\mathfrak{h}}^{n}|_F = \tilde{h}_{\mathfrak{h}}^{n}|_F, \qquad (24)$$

since the value of the Dirichlet data $\omega_{\psi}^{n,p}$ on $\mathscr{I}_{\mathfrak{h}}^{\mathrm{w},n,p}$ is fixed during the loop. This is not the exact continuity of the pressure $\psi = h$ but an $\mathscr{O}(\delta t)$ approximation of it. Furthermore, on the dry part of the interface, the surface water depth is equal to zero and there holds

$$\forall n \leq N_T, \quad \forall F \in \mathscr{I}_{\mathfrak{h}}^{\mathrm{d},n}, \quad \psi_{\mathfrak{h}}^{n}|_F \leq \tilde{h}_{\mathfrak{h}}^{n}|_F. \qquad (25)$$

Again, this is an $\mathscr{O}(\delta t)$ approximation of the condition $\psi \leq 0$. Furthermore, we observe that, if on a given face e_i, the surface water depth h_i^{n-1} is zero as well as the upwind fluxes over the time step $[(n-1)\delta t, n\delta t]$, the Neumann condition on Richards' equation is equal to the rainfall intensity.

On the wet part of $\mathscr{D}$, there holds

$$\forall n \leq N_T, \quad \forall F \in \mathscr{D}_{\mathfrak{h}}^{\mathrm{w},n}, \quad \psi_{\mathfrak{h}}^n|_F = 0 \tag{26}$$

and on the dry part of $\mathscr{D}$, there holds

$$\forall n \leq N_T, \quad \forall F \in \mathscr{D}_{\mathfrak{h}}^{\mathrm{d},n}, \quad v_{\mathfrak{h},\mathscr{D}}^n|_F = 0. \tag{27}$$

As previously, we have only an $\mathscr{O}(\delta t)$ approximation of the condition $\psi \leq 0$ on the dry part of $\mathscr{D}$.
Moreover, we observe that in contrast to front tracking schemes, our algorithm does not use any information from the previous time step to determine the wet portion of the interface. This offers the advantage of robustness and ease of extension to 3D/2D settings, but can entail higher computational costs than those incurred by front tracking schemes in the absence of exfiltration (see for instance [4]).
We present here the main result concerning the overall water volume conservation. Let V^n be the total volume of water contained in the coupled system at time $n\delta t$ defined as

$$V^n = \int_\Omega \theta(\psi_{\mathfrak{h}}^n) + \int_{\mathscr{I}} h_{\mathfrak{h}}^n, \tag{28}$$

let $F_{\mathscr{W}\mathscr{B}\mathscr{D}}^n$ be the flux over $[(n-1)\delta t, n\delta t]$ across the bottom, the lateral walls and the drains,

$$F_{\mathscr{W}\mathscr{B}\mathscr{D}}^n = -\int_{\mathscr{W}\cup\mathscr{B}} v_N^n - \int_{\mathscr{D}} v_{\mathfrak{h},\mathscr{D}}^{\star,n}, \tag{29}$$

and let F_{ABr}^n be the flux over $[(n-1)\delta t, n\delta t]$ due to the rain and the discharge at points A and B,

$$F_{\mathrm{ABr}}^n = \frac{\delta t'}{\delta t}\sum_{k=1}^{n'}\Big(q(h_{\mathrm{A}}^{n-1,k}) - q(h_{N_{\mathscr{I}}}^{n-1,k}) - \int_{\mathscr{I}} v_{\mathrm{r}}^{n-1,k}\cdot n_\Omega\Big). \tag{30}$$

The result concerning the overall water volume conservation is proven in [6].

Property. *Let δV^n be the overall water volume defect over the time step $[(n-1)\delta t, n\delta t]$ defined as*

$$\delta V^n = V^n - V^{n-1} - (\tilde{F}_{\mathscr{W}\mathscr{B}\mathscr{D}}^n + F_{\mathrm{ABr}}^n)\delta t, \tag{31}$$

where $\tilde{F}_{\mathscr{W}\mathscr{B}\mathscr{D}}^n = \frac{2}{3}F_{\mathscr{W}\mathscr{B}\mathscr{D}}^n + \frac{1}{3}\tilde{F}_{\mathscr{W}\mathscr{B}\mathscr{D}}^{n-1}$. Let ΔV^n be the overall water volume defect over the time interval $[0, n\delta t]$ defined as $\Delta V^n = \sum_{i=1}^n \delta V^i$. Then

$$|\Delta V^n| \leq \frac{1}{2}|\delta V^1| + nC\varepsilon, \tag{32}$$

where C is a constant and ε is the user-defined tolerance in the resolution of the non-linear system.

3.4. Validation Test Case

We study a field with buried drainage pipes subjected to a constant rainfall intensity equal to 5mm h^{-1} as indicated on Figure (**7**). The length, the width of the domain and the slope of the interface and the bottom are respectively 32m, 1m and 0.5%. The total simulation time is 3h. The soil is parametrized by the modified Van Genuchten's laws (see §2.3) with parameters,

$\theta_{\mathrm{r}} = 0$	$\theta_{\mathrm{s}} = 0.43$
$K_{\mathrm{s}} = 2.7\ 10^{-4}\mathrm{cm\ s}^{-1}$	$\varepsilon = 0.0094\ \mathrm{cm}^{-1}$
$h_{\mathrm{s}} = 2\mathrm{cm}$	$n = 1.13$
	$m = 0.115.$

Four drains $(\mathrm{d}_1, \mathrm{d}_2, \mathrm{d}_3, \mathrm{d}_4)$, with a diameter equal to $2cm$, are located at $3cm$ above the bottom,

$$c_{\mathrm{d}_1} = (4\mathrm{m}, 17\mathrm{cm}),\ c_{\mathrm{d}_2} = (12\mathrm{m}, 13\mathrm{cm}),$$
$$c_{\mathrm{d}_3} = (20\mathrm{m}, 9\mathrm{cm}),\ c_{\mathrm{d}_4} = (28\mathrm{m}, 5\mathrm{cm}),$$

where $c_{\mathrm{d_i}}$ is the center of drain i $(1 \leq i \leq 4)$. The drain boundaries are denoted $\mathscr{D}_1, \mathscr{D}_2, \mathscr{D}_3$ and $\mathscr{D}_4$. A zero flux is imposed on the lateral walls and bottom,

$$v_N = 0 \text{ on } \mathscr{W}\cup\mathscr{B}\times[0,T]. \tag{33}$$

The Strickler coefficient $\mathscr{K}$ is set to $30m^{1/3}s^{-1}$.

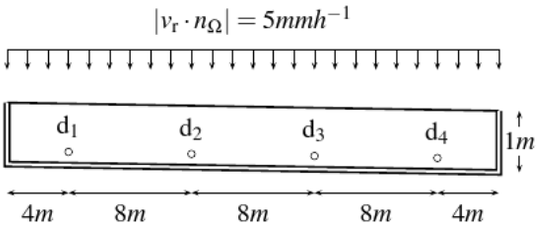

Fig. (**7**): field with four drains.

We consider two initial conditions (IC) for testing the response of the system,

$$\begin{aligned} &\text{IC1:} \quad \psi^0 = -0.5z, \\ &\text{IC2:} \quad \psi^0 = -0.5(z - 0.005(32-x)). \end{aligned} \tag{34}$$

The isolines of ψ are horizontal for IC1 while they are parallel to the bottom for IC2. The water table position is represented on Figures (**8**), (**9**) and (**10**) at 1h, 1h 15min and 1h 30min.
Figures (**8**), (**9**) and (**10**) show that the water table position strongly depends on the initial condition. IC1 leads to different positions between two successive drains whereas IC2 leads to similar positions between two successive drains.

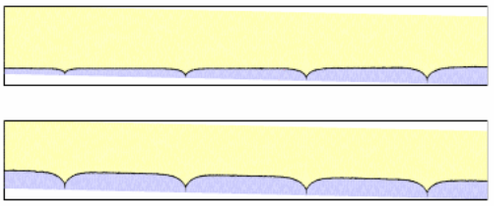

Fig. (**8**): Water table position at 1h IC1 (up) and IC2 (bottom).

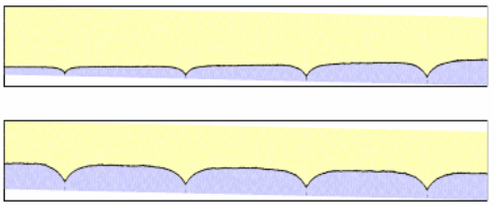

Fig. (**9**): Water table position at 1h 15min IC1 (up) and IC2 (bottom).

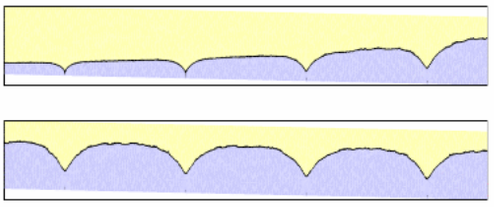

Fig. (**10**): Water table position at 1h 30min IC1 (up) and IC2 (bottom).

We also consider on Figure (**11**) and (**12**) the outflow over the time interval $[(n-1)\delta t, n\delta t]$ on each drain,

$$1 \leq i \leq 4, \quad \mathbb{M}^n_{\mathscr{D}_i} = -\rho\,\delta t \int_{\mathscr{D}_i} v^{\star,n}_{\mathfrak{h},\mathscr{D}_i}, \tag{35}$$

and the total outflow of water

$$\mathbb{M}^n_{\mathscr{D}} = \sum_{i=1}^{4} \mathbb{M}^n_{\mathscr{D}_i}. \tag{36}$$

A difference of 8 minutes between two successive drains is observed on Figure (**11**) leading to a difference of 24 minutes between the first and the last drain. On the other hand, a complete synchronisation is observed on Figure (**12**). These results concerning the initial condition are particularly interested. Isolines of ψ parallel to the bottom are more realistic than horizontal isolines because they match qualitatively experimental observations: a similar water table evolution between two succecutive drains and a synchronization of the fluxes across the drains.

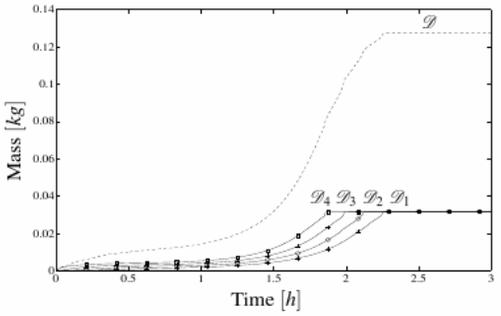

Fig. (**11**): Water fluxes at the drains - IC 1.

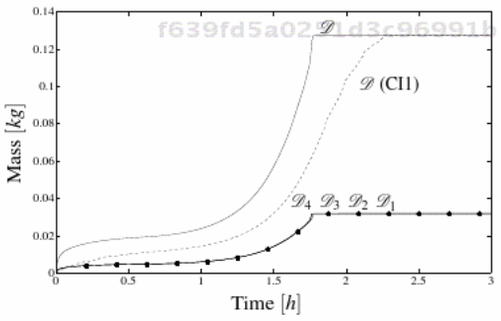

Fig. (**12**): Water fluxes at the drains - IC 2.

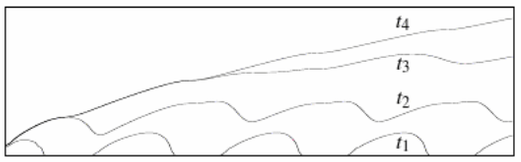

Fig. (**13**): Surface water depth at various times (t_1 = 1h40, t_2 = 1h47, t_3 = 1h55 and t_4 = 3h).

The surface water depth (obtained with IC2) represented at various times on Figure (**13**) shows that our algorithm is able 1) to account for multiple exfiltration zones at the interface and 2) to connect these wet zones.

3.5. Optimization

One drawback of Algorithm 1 is that two iterations are necessary to evaluate the partition of the interface when the surface water is totally absorbed by the soil. For the test case previously presented, Figure (**14**) shows the number of iterations to determine the partition of the interface (note that a Dirichlet condition is imposed on the drains and the partition of $\mathscr{D}_\mathfrak{h}$ is not considered here) and the number of Dirichlet faces on the interface. It is clear that two iterations are needed for infiltrating the water

until 1h 40min.

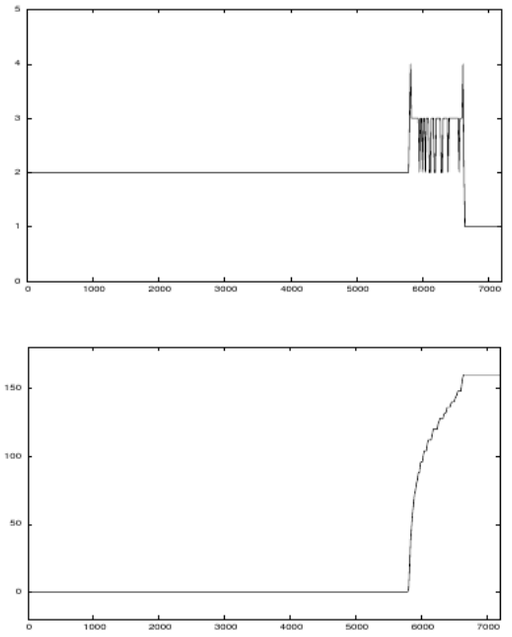

Fig. (**14**): Number of iterations (top) - number of Dirichlet faces on $\mathscr{I}_\mathfrak{h}$ (bottom) with Algorithm 1.

To reduce the number of iterations when a Neumann condition is imposed on all the faces of the interface, we propose an adaptation of Algorithm 1.
Algorithm 2 is based on two choices to impose the boundary conditions on the interface:

1. When there exists one face of the interface with a Dirichlet condition at time $(n-1)\delta t$, the condition $\max(\psi_\mathfrak{h}^{n,0}|_\mathscr{I}) \geq 0$ is immediately verified because $\psi_\mathfrak{h}^{n,0}|_\mathscr{I} = \psi_\mathfrak{h}^{n-1}|_\mathscr{I}$ and a partition of the interface is required.

2. When no face of the interface has a Dirichlet condition at time $(n-1)\delta t$, the condition $\max(\psi_\mathfrak{h}^{n,0}|_\mathscr{I}) \geq 0$ is not verified and there is no partition of the interface as $\mathscr{I}_\mathfrak{h}^{\mathrm{d},n,p} = \mathscr{I}_\mathfrak{h}$. We assume that the surface water is totaly infiltrated owing to the Neumann condition $\omega_v^{n,p} = -\tilde{h}_\mathfrak{h}^n/\delta t$. Two cases are possible: either the water is effectively absorbed in the soil or the water is not completely absorbed. In the first case ($\max(\psi_\mathfrak{h}^{n,0}|_\mathscr{I}) < 0$), only one iteration is necessary to converge (instead of two with Algorithm 1). In the second case ($\max(\psi_\mathfrak{h}^{n,0}|_\mathscr{I}) \geq 0$), the algorithm swaps to the choice 1 because a partition of the interface is required.

Figure (**15**) shows the number of iterations and the number of Dirichlet faces on the interface with Algorithm 2. As expected, the number of iterations

Algorithm 2 Coupling algorithm with the choice of the interface partition

Require: $\psi_\mathfrak{h}^{n-1}$ and $h_\mathfrak{h}^{n-1}$

$\tilde{h}_\mathfrak{h}^n \leftarrow \mathtt{KW}(h_\mathfrak{h}^{n-1}, n', v_\mathrm{r}^{n-1}, 0)$

Set $p = 0$ and $h_\mathfrak{h}^{n,0} = \tilde{h}_\mathfrak{h}^n$,

Set $\psi_\mathfrak{h}^{n,0}|_\mathscr{I} = \psi_\mathfrak{h}^{n-1}|_\mathscr{I}$,

Set $\psi_\mathfrak{h}^{n,0}|_\mathscr{D} = 0$ and $v_{\mathfrak{h},\mathscr{D}}^{\star,n,0} = 0$,

repeat

$p \leftarrow p+1$

if $\max(\psi_\mathfrak{h}^{n,p-1}|_\mathscr{I}) \geq 0$ **then**

$\{\mathscr{I}_\mathfrak{h}^{\mathrm{d},n,p}, \mathscr{I}_\mathfrak{h}^{\mathrm{w},n,p}\} \leftarrow \mathtt{I\_Part}(h_\mathfrak{h}^{n,0}, \ldots, h_\mathfrak{h}^{n,p-1})$

$\{\mathscr{D}_\mathfrak{h}^{\mathrm{d},n,p}, \mathscr{D}_\mathfrak{h}^{\mathrm{w},n,p}\} \leftarrow \mathtt{D\_Part}(\psi_\mathfrak{h}^{n,0}, \ldots, \psi_\mathfrak{h}^{n,p-1})$

$\{\omega_v^{n,p}, \omega_\psi^{n,p}\} \leftarrow \mathtt{I\_BC}(\tilde{h}_\mathfrak{h}^n, \mathscr{I}_\mathfrak{h}^{\mathrm{d},n,p}, \mathscr{I}_\mathfrak{h}^{\mathrm{w},n,p})$

$\psi_\mathfrak{h}^{n,p} \leftarrow \mathtt{Ric\_BDF2}(\mathscr{I}_\mathfrak{h}^{\mathrm{d},n,p}, \mathscr{I}_\mathfrak{h}^{\mathrm{w},n,p}, \omega_v^{n,p}, \omega_\psi^{n,p})$

$v_{\mathfrak{h},\mathscr{I}}^{\star,n,p} \leftarrow \mathtt{Velocity}(\mathscr{I}_\mathfrak{h}^{\mathrm{d},n,p}, \mathscr{I}_\mathfrak{h}^{\mathrm{w},n,p}, \omega_v^{n,p}, \omega_\psi^{n,p})$

$v_{\mathfrak{h},\mathscr{D}}^{\star,n,p} \leftarrow \mathtt{Velocity}(\mathscr{D}_\mathfrak{h}^{\mathrm{d},n,p}, \mathscr{D}_\mathfrak{h}^{\mathrm{w},n,p}, 0, 0)$

$\forall\, F \in \mathscr{I}_\mathfrak{h}$,

$h^{n,p}|_F = \tilde{h}^n|_F + \delta t/|F| \int_F (2v_{\mathfrak{h},\mathscr{I}}^{\star,n,p} + v_{\mathfrak{h},\mathscr{I}}^{\star,n-1})/3$

else

$\mathscr{I}_\mathfrak{h}^{\mathrm{d},n,p} = \mathscr{I}_\mathfrak{h}$ and $\mathscr{I}_\mathfrak{h}^{\mathrm{w},n,p} = \emptyset$

$\{\mathscr{D}_\mathfrak{h}^{\mathrm{d},n,p}, \mathscr{D}_\mathfrak{h}^{\mathrm{w},n,p}\} \leftarrow \mathtt{D\_Part}(\psi_\mathfrak{h}^{n,0}, \ldots, \psi_\mathfrak{h}^{n,p-1})$

$\omega_v^{n,p} = -\tilde{h}_\mathfrak{h}^n/\delta t$

$\psi_\mathfrak{h}^{n,p} \leftarrow \mathtt{Ric\_BDF2}(\mathscr{I}_\mathfrak{h}^{\mathrm{d},n,p}, \mathscr{I}_\mathfrak{h}^{\mathrm{w},n,p}, \omega_v^{n,p}, \omega_\psi^{n,p})$

$v_{\mathfrak{h},\mathscr{D}}^{\star,n,p} \leftarrow \mathtt{Velocity}(\mathscr{D}_\mathfrak{h}^{\mathrm{d},n,p}, \mathscr{D}_\mathfrak{h}^{\mathrm{w},n,p}, 0, 0)$

$\forall\, F \in \mathscr{I}_\mathfrak{h}, h^{n,p}|_F = 0$

end if

until 1 - $\forall\, F \in \mathscr{I}_\mathfrak{h}, h^{n,p}|_F \geq 0$

2 - $\forall\, F \in \mathscr{D}_\mathfrak{h}, v_{\mathfrak{h},\mathscr{D}}^{\star,n,p}|_F \geq 0$

Ensure: $\psi_\mathfrak{h}^n = \psi_\mathfrak{h}^{n,p}$ and $h_\mathfrak{h}^n = h_\mathfrak{h}^{n,p}$

is one until 1h 40min. The same evolution in time of the number of Dirichlet faces on the interface is obtained with Algorithm 1 and Algorithm 2. In this case where there is a substantial period of time without surface runoff, Algorithm 2 allows to reduce the CPU time by a factor two.

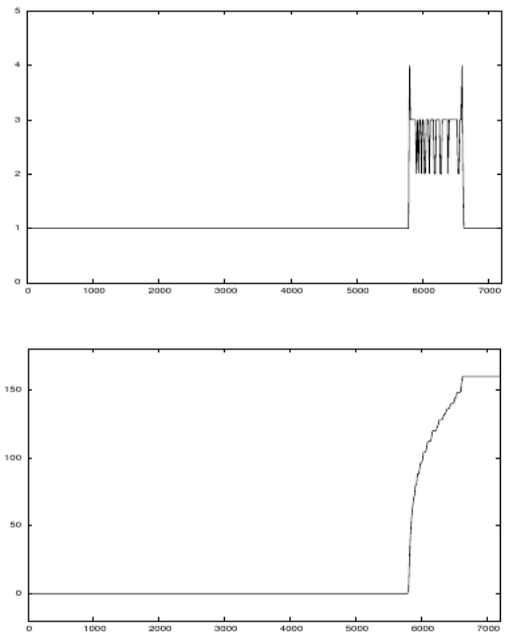

Fig. (**15**): Number of iterations (top) - number of Dirichlet faces on $\mathscr{I}_\mathfrak{h}$ (bottom) with Algorithm 2.

CONCLUSIONS

In this chapter we have presented a robust and accurate algorithm to simulate coupled subsurface and overland flows governed by Richards' equation and the kinematic wave equation. Special care was taken to design interface fluxes that preserve the overall water volume in the system and that satisfy the various equality and inequality constraints imposed at the interface and around the drains. Additional hydrological test cases (with heterogeneous soil for instance) should be envisaged. Extension to two-dimensional surface flows and three-dimensional subsurface variably saturated flows can also be considered. A further possible extension is to account for the topography evolution by means of the Exner equation.

REFERENCES

[1] Beavers G, Joseph D. Boundary conditions at a naturally impermable wall. J Fluid Mech 1967; 30: 197-207.
[2] Saffman PG. On the boundary condition at the interface of a porous medium. Stud Appl Math 1971; 1: 93-101.
[3] VanderKwaak JE, Loague K. Hydrologic-response simulations for the R-5 catchment with a comprehensive physics-based model. Water Resources Res 2001; 37: 999-1013,
[4] Beaugendre H, A. Ern A, Esclaffer T, Gaume E, Ginzburg I, Kao C. A seepage face model for the interaction of shallow water tables with the ground water surface: Application of the obstacle-type method. J Hydrology 2006; 329: 258-273.
[5] Dawson C. Analysis of Discontinuous finite element methods for ground water/surface water coupling. SIAM J Numer Anal 2006; 44: 1375-1404.
[6] Sochala P, Ern A, Piperno S. Mass conservative BDF-discontinuous Galerkin/explicit finite volume schemes for coupling subsurface and overland flows. Comput Meth Appl Mech Engrg 2009; 198: 2122-2136.
[7] Vogel T, Van Genuchten M.Th, Cislerova M. Effect of the shape of the soil hydraulic functions near saturation on variably-saturated flow predictions. Adv Water Resources 2001; 24: 133-144.
[8] Cuthill E, McKee J. Reducing the bandwidth of sparse symmetric matrices. Naval Ship Research and Development Center. Washington, D.C. 2007.
[9] Ern A, Nicaise S, Vohralík M. An accurate $H(\mathrm{div})$ flux reconstruction for discontinuous Galerkin approximations of elliptic problems. CR Math Acad Sci Paris 2007; 345: 709-712.